

# The chord-length probability density of the regular octahedron

Salvino Ciccariello

*Università di Padova, Dipartimento di Fisica G. Galilei  
Via Marzolo 8, I-35131 Padova, Italy  
salvino.ciccariello@unipd.it*

January 16, 2014  
revised February 8, 2014

## Abstract

The chord length probability density of the regular octahedron is explicitly evaluated throughout its full range of distances by separating it into three contributions respectively due to the pairs of facets opposite to each other or sharing an edge or a vertex.

# 1 Introduction

Small-angle scattering<sup>1–3</sup> (SAS) is a powerful tool to get information on the interface size and shape of a sample. In fact, the observed scattering intensity is the square modulus of the Fourier transform (FT) of  $n(\mathbf{r})$ , the scattering density of the sample, or, equivalently, the FT of the convolution of  $n(\mathbf{r})$  by itself. In the SAS realm  $n(\mathbf{r})$  can fairly be approximated by a discrete value function that takes only two values in most of the cases. This approximation implies that the sample is either a bi-continuous or a particulate system. Confining ourselves to the second case, if one further assumes that particles have the same shape and size, that are isotropically distributed and that their number density is small (conditions fairly met in the case of biological samples), then the scattering density is proportional to the FT of the isotropic correlation function of the particle defined as

$$\gamma(r) \equiv (1/4\pi V) \int d\hat{\omega} \int \rho_V(\mathbf{r}_1) \rho_V(\mathbf{r}_1 + r\hat{\omega}) dv_1. \quad (1)$$

Here  $\rho_V(\mathbf{r})$  denotes the characteristic function of set  $\mathcal{V}$  (having volume  $V$ ) occupied by the particle (*i.e.* it is defined as being equal to one inside the particle and to zero elsewhere). Further, the inner integral is performed over  $\mathcal{V}$  (or the all space) and the outer integral over all the directions of the unit vector  $\hat{\omega}$ .

As first pointed out by Debye *et al.*<sup>4</sup>, the right hand side of (1), suitably scaled, can be interpreted as the probability density that by randomly tossing a stick of length  $r$  both ends of the stick fall within the particle. This remark shows the stochastic meaning of  $\gamma(r)$ . Consequently, SAS theory is intimately related to stochastic geometry<sup>5</sup> as well as to integral geometry<sup>6</sup> that aims to get general properties investigating suitable integrals over the particle volume or surface. Interestingly, the derivatives of  $\gamma(r)$  can be expressed as integrals over the particle surface<sup>7,8</sup> and, in the case of convex particles, the first and second derivatives (after being appropriately scaled) can be interpreted as the probability densities for respectively finding the stick with one end or with both ends on the particle surface. The investigations of these integral relations yield some general result as the Porod<sup>9</sup> and the Kirste-Porod<sup>10</sup> relations as well as the particle surface features that yield discontinuous  $\gamma''(r)$ s<sup>11–13</sup>.

These considerations illustrate the importance of determining the explicit expressions of  $\gamma(r)$ ,  $\gamma'(r)$  or  $\gamma''(r)$  for specific particle shapes. In fact, these expressions were obtained in the cases of spheres<sup>2</sup>, cubes<sup>14</sup>, cylinders<sup>15</sup>, right parallelepipeds<sup>16</sup>, rotational ellipsoids<sup>17</sup> and regular tetrahedrons<sup>18</sup>.

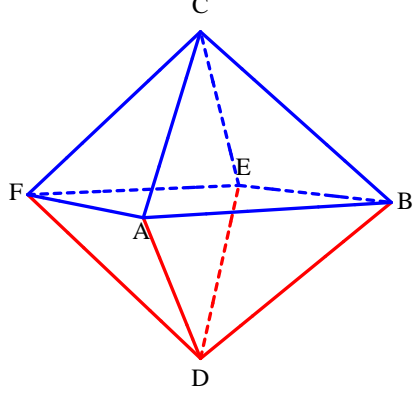


Figure 1: The regular octahedron.

This paper goes one step further since it determines the chord-length probability density  $\mathcal{C}(r)$  of another Platonic solid: the regular octahedron (see Fig. 1).

## 2 Basic integral expression

In order to evaluate  $\mathcal{C}(r)$  one starts from the general integral expression of  $\gamma''(r)$  obtained by Ciccariello *et al.*<sup>7</sup>, namely

$$\gamma''(r) = -\frac{1}{4\pi V} \int d\hat{\omega} \int_{S_1} dS_1 \int_{S_2} dS_2 (\hat{\nu}_1(\mathbf{r}_1) \cdot \hat{\omega})(\hat{\nu}_2(\mathbf{r}_2) \cdot \hat{\omega}) \delta(\mathbf{r}_1 + r\hat{\omega} - \mathbf{r}_2). \quad (2)$$

Here  $S_1 = S_2 = S$  and  $V$  respectively denote the surface and volume of the octahedron,  $\hat{\nu}_1(\mathbf{r}_1)$  [ $\hat{\nu}_2(\mathbf{r}_2)$ ] the unit normal (pointing outwardly to the octahedron) to the infinitesimal surface element  $dS_1$  [ $dS_2$ ] of  $S$ , located at the point with position vector  $\mathbf{r}_1$  [ $\mathbf{r}_2$ ]. The Dirac function  $\delta(\cdot)$ , present in (2), requires that the distance between  $dS_1$  and  $dS_2$  be equal to  $r(\geq 0)$  since  $\hat{\omega}$  denotes a unit vector which, according to the leftmost integral of (2), ranges over all the possible directions. Thus, at fixed  $dS_1$ , the integrals over  $d\hat{\omega}$  and  $dS_2$  amounts to integrating over the curve resulting from the intersection of the sphere of radius  $r$  and centered at  $dS_1$  with  $S$ .

To explicitly evaluate expression (2) it is convenient to account for the fact that  $S$  is formed by eight triangular faces. Thus, expression (2) reduces to a sum of terms having still the form of (2) but with the important changes

that integration domains  $S_1$  and  $S_2$  are two facets of the octahedron. Clearly the only cases where  $S_1$  and  $S_2$  are different is important, otherwise the correspondent integrand vanishes because  $\hat{\omega}$  is perpendicular both to  $\hat{\nu}_1$  and  $\hat{\nu}_2$ . Then, for each couple  $(S_1, S_2)$ , the facets share an edge or a vertex or, in the negative case, they lie oppositely and the associated planes are parallel. In the last case, for conciseness, the facets will be said parallel. For each couple  $(S_1, S_2)$ , expression (2) defines a scalar  $r$ -function. Hence, whatever  $S_1$  and  $S_2$ , expression (2) takes the same form, denoted by  $\gamma_E''(r)$ , if  $S_1$  and  $S_2$  share an edge. The same happens if  $S_1$  and  $S_2$  share a vertex or are parallel and the corresponding integrals will be denoted by  $\gamma_V''(r)$  and  $\gamma_P''(r)$ , respectively. Thus, it results that

$$\gamma''(r) = 24\gamma_E''(r) + 24\gamma_V''(r) + 8\gamma_P''(r), \quad (3)$$

and the evaluation of  $\gamma''(r)$  reduces to that of  $\gamma_E''(r)$ ,  $\gamma_V''(r)$  and  $\gamma_P''(r)$ . The evaluations will be carried out in the following three sections assuming that the edge length  $\ell$  of the octahedrons be equal to one. This assumption is by no way restrictive. In fact, if one respectively denotes by  $\gamma_\ell''(r)$  and  $\gamma''(r)$  the functions relevant to the octahedrons with edges equal to  $\ell$  and 1, one has  $\gamma_\ell''(r) = (1/\ell^2)\gamma''(r/\ell)$ .

### 3 Evaluation of $\gamma_E''(r)$

The geometrical configuration relevant to  $\gamma_E''(r)$  is shown in Fig. 2. Surfaces  $S_1$  and  $S_2$  respectively are the regular triangles ABC and ABD with unit sides. It is now put

$$\beta = \hat{BAC} = \pi/3, \quad \alpha = \hat{DOC} = \arccos(-1/3), \quad \alpha_c = \pi - \alpha, \quad (4)$$

$$H = OC = OD = \frac{\sqrt{3}}{2}, \quad h = D_0D = H \sin \alpha_c = \sqrt{\frac{2}{3}}, \quad |DC| = \sqrt{2}. \quad (5)$$

The minimax distances<sup>11</sup> are

$$d_1 = h, \quad d_2 = H, \quad d_3 = 1 \quad \text{and} \quad d_4 = \sqrt{2}. \quad (6)$$

In terms of the axes shown in Fig. 2, one has

$$dS_1 = dx \, dz \quad \text{and} \quad dS_2 = dY \, dZ. \quad (7)$$

The integration domain of  $dS_1$  (*i.e.* the triangle ABC) is defined by the inequalities

$$0 < x < H \quad \text{and} \quad -L_E(x) < z < L_E(x), \quad (8)$$



The  $x$ ,  $Y$  and  $Z$  integrals are immediately performed and, taking into account that the Jacobian related to the  $Y$  variable is  $1/\sin \alpha$ , one finds that

$$\gamma_E''(r) = -\frac{1}{4\pi V \sin \alpha} \int_0^\pi d\theta \int_{-\frac{\pi-\alpha}{2}}^{\frac{\pi-\alpha}{2}} A_E(\theta, \varphi) \Theta_E(\bar{x}, \bar{Y}) d\varphi \int_{-L_E(\bar{x})}^{L_E(\bar{x})} \Theta_z(\bar{Z}) dz, \quad (14)$$

where function  $\Theta_E(\bar{x}, \bar{Y})$ , depending on  $\theta$  and  $\varphi$ , is equal to one if  $\bar{x}$  and  $\bar{Y}$  obey inequalities (8a) and (9a) and to zero elsewhere. Similarly  $\Theta_z(\bar{Z})$  is equal to one or zero depending on whether  $\bar{Z}$  obeys inequalities (9b) or not. According to (13a)  $\bar{Z}$  linearly depends on  $z$ . Then, the above  $z$ -integral is equal to

$$F_E(r, \theta, \varphi) \equiv \min[L_E(\bar{x}), L_E(\bar{Y}) - r \cos \theta] - \max[-L_E(\bar{x}), -L_E(\bar{Y}) - r \cos \theta] = \min[L_E(\bar{x}), L_E(\bar{Y}) - r \cos \theta] + \min[L_E(\bar{x}), L_E(\bar{Y}) + r \cos \theta] \quad (15)$$

if the above quantity is positive otherwise it is equal to zero. It is now observed that each of the following transformations  $\theta \rightarrow (\pi - \theta)$  and  $\varphi \rightarrow -\varphi$  interchanges  $\bar{x}$  with  $\bar{Y}$  and leaves expressions (12) and (15) invariant. Thus, (14) becomes

$$\gamma_E''(r) = -\frac{1}{\pi V \sin \alpha} \int_0^{\pi/2} d\theta \int_0^{(\pi-\alpha)/2} A_E(\theta, \varphi) F_E(r, \theta, \varphi) d\varphi, \quad (16)$$

with the constraints

$$0 < \bar{x}(r, \theta, \varphi) < H, \quad 0 < \bar{Y}(r, \theta, \varphi) < H, \quad F_E(r, \theta, \varphi) > 0 \quad (17)$$

that will generally reduce the integration domain

$$\mathcal{D}_E \equiv \{0 < \theta < \pi/2, \quad 0 < \varphi < (\pi - \alpha)/2\} \quad (18)$$

to a smaller one. All the constraints must explicitly be reduced in order to get the explicit expression of  $\gamma_E''(r)$ . To this aim we start from the constraints implicit in definition (15). Putting

$$\mu_\pm(\theta, \varphi) \equiv 2 \operatorname{ctg} \beta \sin \theta \cos(\varphi \pm \alpha/2) / \sin \alpha \quad (19)$$

one easily shows that  $F_E(r, \theta, \varphi)$  becomes

$$F_E(r, \theta, \varphi) = 1 - \frac{r}{2} (\max[\mu_+ + \cos \theta, \mu_- - \cos \theta] + \max[\mu_+ - \cos \theta, \mu_- + \cos \theta]). \quad (20)$$

The condition  $(\mu_+ + \cos \theta) > (\mu_- - \cos \theta)$  is fulfilled within the  $\mathcal{D}_E$  sub-domain

$$\mathcal{D}_{E,A} \equiv \{0 < \varphi < (\pi - \alpha)/2, \quad 0 < \theta < \bar{\theta}_E(\varphi) \equiv \operatorname{arctg}(\sin \varphi)\}, \quad (21)$$

and  $(\mu_- + \cos \theta) > (\mu_+ - \cos \theta)$  throughout  $\mathcal{D}_E$ . Then, from equations (20) and (4) follows that  $F_E(r, \theta, \varphi)$  takes the forms

$$F_{E,A}(r, \theta, \varphi) \equiv 1 - r \left( \cos \theta + \frac{\sin \theta \cos \varphi}{\sqrt{2}} \right) \quad \text{if } (\theta, \varphi) \in \mathcal{D}_{E,A}, \quad (22)$$

and

$$F_{E,B}(r, \theta, \varphi) \equiv 1 - r \sqrt{3/2} \sin \theta \cos(\varphi - \alpha/2) \quad \text{if } (\theta, \varphi) \in \mathcal{D}_{E,B}, \quad (23)$$

$\mathcal{D}_{E,B}$  being defined as the complementary domain of  $\mathcal{D}_{E,A}$  in  $\mathcal{D}_E$ .

### 3.1 Constraints and integration domains

Before proceeding to the integral evaluation one must still reduce inequalities (17a), (17b) and (17c). The last requires that  $F_{E,A} > 0$  within  $\mathcal{D}_{E,A}$  and that  $F_{E,B} > 0$  within  $\mathcal{D}_{E,B}$ . The inequalities depend on  $r$  and the same will happen for the associated domains that will be determined confining ourselves to  $\mathcal{D}_E$  and to the non-trivial  $r$ -domain  $[0, \sqrt{2}]$  of  $\gamma''(r)$ .

For inequalities (17a) one finds that the associated domain  $\mathcal{D}_{E,x}(r)$  is

$$\mathcal{D}_{E,x}(r) = \mathcal{D}_E \quad \text{if } 0 < r < \sqrt{3}/2, \quad (24)$$

$$\mathcal{D}_{E,x}(r) = \mathcal{D}_{E,x,1}(r) \cup \mathcal{D}_{E,x,2}(r) \quad \text{if } \sqrt{3}/2 < r < \sqrt{2}, \quad (25)$$

with

$$\mathcal{D}_{E,x,1}(r) \equiv \{0 < \theta < \pi/2, 0 < \varphi < \bar{\phi}_{E,x}(r)\}, \quad (26)$$

$$\mathcal{D}_{E,x,2}(r) \equiv \{\bar{\phi}_{E,x}(r) < \varphi < (\pi - \alpha)/2, 0 < \theta < \bar{\theta}_{E,x}(r, \varphi)\}, \quad (27)$$

and

$$\bar{\phi}_{E,x}(r) \equiv \alpha/2 - \arccos(\sqrt{2/3}/r), \quad (28)$$

$$\bar{\theta}_{E,x}(r, \varphi) \equiv \arcsin(\sqrt{2/3}/[r \cos(\varphi - \alpha/2)]). \quad (29)$$

Inequalities (17b) are fulfilled throughout  $\mathcal{D}_E$  if  $0 < r < \sqrt{2}$ .

Inequality  $F_{E,B}(r, \theta, \varphi) > 0$  coincides with  $\bar{x}(r, \theta, \varphi) < H$  and is therefore obeyed throughout  $\mathcal{D}_{E,F_B} \equiv \mathcal{D}_{E,x}$ .

The reduction of the last inequality  $F_{E,A}(r, \theta, \varphi) > 0$  yields the domain  $\mathcal{D}_{E,F_A}(r)$  defined as

$$\mathcal{D}_{E,F_A,a}(r) \equiv \mathcal{D}_{E,A} \quad \text{if } 0 < r < \sqrt{2/3}, \quad (30)$$

to

$$\mathcal{D}_{E,FA,b}(r) = \begin{cases} \mathcal{D}_{E,A,1}(r) \equiv \{0 < \theta < \mathcal{L}_{E,1}(r), & 0 < \varphi < (\pi - \alpha)/2\}, \\ \mathcal{D}_{E,A,2}(r) \equiv \{\mathcal{L}_{E,1}(r) < \theta < \mathcal{L}_{E,2}(r), & \bar{\phi}_{E,A}(r, \theta) < \varphi < (\pi - \alpha)/2\} \\ \mathcal{D}_{E,A,3}(r) \equiv \{\mathcal{L}_{E,2}(r) < \theta < \pi/2, & 0 < \varphi < (\pi - \alpha)/2\}, \end{cases} \quad (31)$$

if  $\sqrt{2/3} < r < \sqrt{3}/2$ , to

$$\mathcal{D}_{E,FA,c}(r) = \begin{cases} \mathcal{D}_{E,A,1}(r), \\ \mathcal{D}'_{E,A,2}(r) \equiv \{\mathcal{L}_{E,1}(r) < \theta < \mathcal{L}_{E,3}(r), & \bar{\phi}_{E,A}(r, \theta) < \varphi < (\pi - \alpha)/2\}, \\ \mathcal{D}'_{E,A,3}(r) \equiv \{\mathcal{L}_{E,4}(r) < \theta < \mathcal{L}_{E,2}(r), & \bar{\phi}_{E,A}(r, \theta) < \varphi < (\pi - \alpha)/2\}, \\ \mathcal{D}'_{E,A,4}(r) \equiv \{\mathcal{L}_{E,2}(r) < \theta < \pi/2, & 0 < \varphi < (\pi - \alpha)/2\} \end{cases} \quad (32)$$

if  $\sqrt{3}/2 < r < 1$ , and to

$$\mathcal{D}_{E,FA,d}(r) = \begin{cases} \mathcal{D}''_{E,A,1}(r) \equiv \{\mathcal{L}_{E,4}(r) < \theta < \mathcal{L}_{E,2}(r), & \bar{\phi}_{E,A}(r, \theta) < \varphi < (\pi - \alpha)/2\}, \\ \mathcal{D}''_{E,A,2}(r) \equiv \{\mathcal{L}_{E,2}(r) < \theta < \pi/2, & 0 < \varphi < (\pi - \alpha)/2\} \end{cases} \quad (33)$$

if  $1 < r < \sqrt{2}$ . The involved  $\mathcal{L}_{..}(r)$  functions are defined as follows

$$\mathcal{L}_{E,1}(r) \equiv \bar{\theta}_{E,A,1}(r) - \alpha/2, \quad \mathcal{L}_{E,2}(r) \equiv \pi - \alpha/2 - \bar{\theta}_{E,A,1}(r) \quad (34)$$

$$\mathcal{L}_{E,3}(r) \equiv \bar{\theta}_{E,A,2}(r) - \pi/3, \quad \mathcal{L}_{E,4}(r) \equiv 2\pi/3 - \bar{\theta}_{E,A,2}(r) \quad (35)$$

with

$$\bar{\theta}_{E,A,1}(r) \equiv \arcsin(\sqrt{2/3}/r), \quad (36)$$

$$\bar{\theta}_{E,A,2}(r) \equiv \arcsin(\sqrt{3}/2r), \quad (37)$$

$$\bar{\phi}_{E,A}(r, \theta) \equiv \arccos(\sqrt{2}(1 - r \cos \theta)/(r \sin \theta)). \quad (38)$$

### 3.2 $\gamma_E''(r)$ expression

The  $\gamma_E''(r)$  expression is given by the sum of the following two expressions

$$\gamma_{E,A}''(r) \equiv -\frac{1}{\pi V \sin \alpha} \int_{\bar{\mathcal{D}}_{E,A}(r)} A_E(\theta, \varphi) F_{E,A}(r, \theta, \varphi) d\theta d\varphi \quad (39)$$

$$\gamma_{E,B}''(r) \equiv -\frac{1}{\pi V \sin \alpha} \int_{\bar{\mathcal{D}}_{E,B}(r)} A_E(\theta, \varphi) F_{E,B}(r, \theta, \varphi) d\theta d\varphi \quad (40)$$

with

$$\bar{\mathcal{D}}_{E,A}(r) \equiv \mathcal{D}_{E,FA} \cap \mathcal{D}_{E,x}(r) \cap \mathcal{D}_{E,A}(r) \quad (41)$$

$$\bar{\mathcal{D}}_{E,B}(r) \equiv \mathcal{D}_{E,B} \cap \mathcal{D}_{E,x}(r). \quad (42)$$



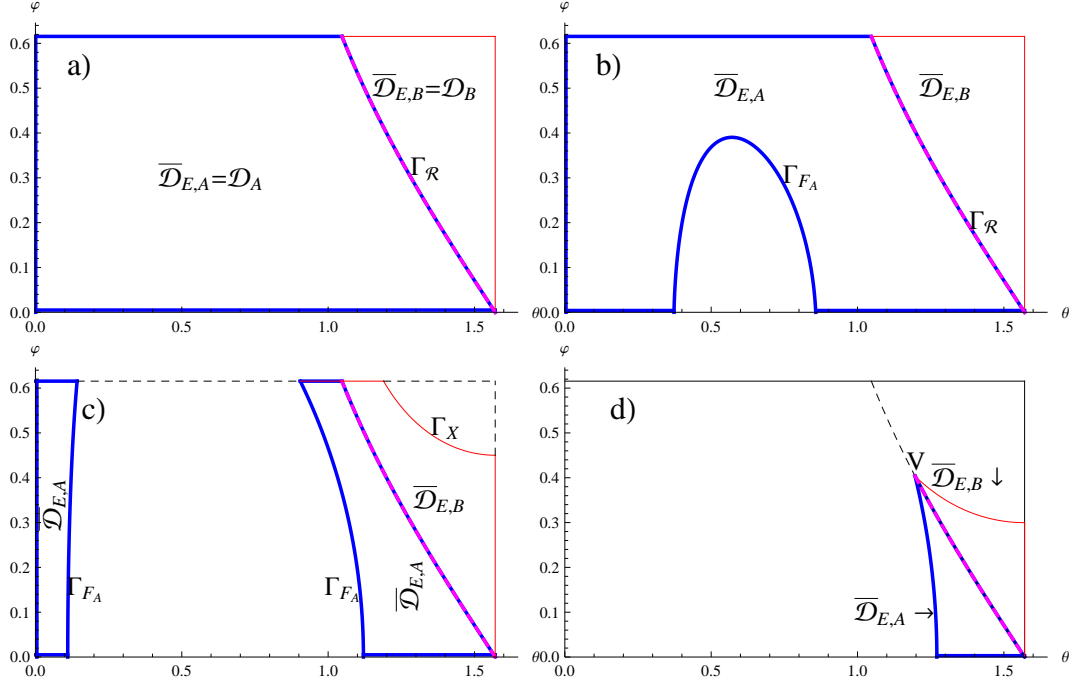


Figure 3: The four panels shows the shapes of the integration domains  $\bar{\mathcal{D}}_{E,A}(r)$  and  $\bar{\mathcal{D}}_{E,B}(r)$  in the four  $r$ -ranges:  $a = [0, \sqrt{2/3}]$ ,  $b = [\sqrt{2/3}, \sqrt{3}/2]$ ,  $c = [\sqrt{3}/2, 1]$  and  $d = [1, \sqrt{2}]$ . The  $\bar{\mathcal{D}}_{E,A}(r)$  domains are bounded by thick blue lines and the  $\bar{\mathcal{D}}_{E,B}(r)$ s by red continuous ones. The dotted thick curve  $\Gamma_R$  separates domain  $\mathcal{D}_{E,F_A}$  from  $\mathcal{D}_{E,F_B}$  and is defined by Eq. (21). The bell shaped curve  $\Gamma_{F_A}$  is related to the condition  $F_{E,A} > 0$  [see Eq.s (31)-(33)] and curve  $\Gamma_x$  to the boundary of  $\mathcal{D}_{E,x}$  [see Eq.s (24)-(29)].

The shapes of these domains are shown in Fig. 3 in the four ranges of distances  $a$ ,  $b$ ,  $c$  and  $d$ , defined in the caption. The evaluation of the integrals is a long task that was made possible by the MATHEMATICA software. By

these results the final  $\gamma_E''(r)$  expression is

$$\gamma_{E,a}''(r) \equiv \frac{2\sqrt{2} - \pi + \alpha}{8\pi} - \frac{(18 + (7\sqrt{3} - 9)\pi)r}{96\sqrt{2}\pi}, \quad (43)$$

$$\gamma_{E,b}''(r) \equiv \frac{1}{12\sqrt{6}r^3} - \frac{1}{2\sqrt{6}r} + \frac{4 + \sqrt{2}(\pi + \alpha)}{8\sqrt{2}\pi} - \frac{(18 - (9 - 13\sqrt{3})\pi)r}{96\sqrt{2}\pi}, \quad (44)$$

$$\begin{aligned} \gamma_{E,c}''(r) \equiv & -\frac{1}{288\sqrt{2}\pi r^3} \left[ -4\sqrt{3}\pi - 36(4 + \sqrt{2}\alpha)r^3 + 3(18 - 9\pi + 10\sqrt{3}\pi)r^4 + \right. \\ & 6(25r^2 - 6)R_{34}(r) + 8\sqrt{3}\arcsin\left[\frac{9r^2 - 7}{2R_{23}^3(r)}\right] + \\ & 96\sqrt{3}r^2\arcsin\left[\frac{1}{2R_{23}(r)}\right] - 72\sqrt{2}r^3\arcsin\left[\frac{r}{\sqrt{3}R_{23}(r)}\right] - \\ & \left. 18\sqrt{3}r^4\arcsin\left[\frac{\sqrt{3}(27 - 90r^2 + 96r^4 - 34r^6 + 2r^8)}{2r^7R_{23}(r)}\right] \right], \end{aligned} \quad (45)$$

$$\begin{aligned} \gamma_{E,d}''(r) \equiv & -\frac{1}{192\pi r^3} \left[ -16\sqrt{2} + 8\sqrt{2}(3 + \sqrt{3}\pi)r^2 - 12\pi r^3 + \right. \\ & 3\sqrt{2}(4\sqrt{3} - 3)\pi r^4 - 4\sqrt{2}(5r^2 - 2)R_{11}(r) - \\ & 24r^3\arcsin\left[\frac{4 + 4r^2 - 7r^4}{R_{23}^4(r)}\right] + 36\sqrt{2}r^4\arcsin\left[\frac{R_{11}(r)}{r}\right] - \\ & \left. 8\sqrt{6}r^2(2 + 3r^2)\arcsin\left[\frac{1 + 3R_{11}(r)}{2R_{23}(r)}\right] \right]. \end{aligned} \quad (46)$$

Here suffices  $a, b, c$  and  $d$  specify the  $r$ -range where the expressions apply and the following definitions have also been used

$$R_{11}(r) = \sqrt{r^2 - 1}, \quad R_{23}(r) = \sqrt{3r^2 - 2}, \quad R_{34}(r) = \sqrt{4r^2 - 3}. \quad (47)$$

## 4 Evaluation of $\gamma_V''(r)$

One passes now to evaluate the CLPD relevant to a pair of facets sharing a vertex. The configuration is shown in Fig. 4 that also shows the Cartesian frames used to work out the CLPD expression. The evaluation proceeds along the same route described in section 3. The integration domains  $S_1 = ABC$  and  $S_2 = CEF$  are defined by the inequalities

$$0 < x < H, \quad -L_V(x) < z < L_V(x) \quad (48)$$

and

$$0 < Y < H, \quad -L_V(Y) < Z < L_V(Y) \quad (49)$$

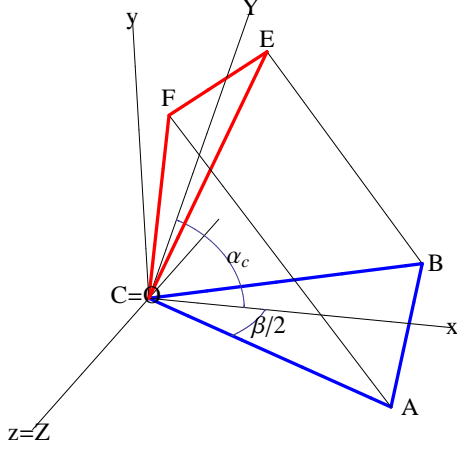


Figure 4: Cartesian frames used for evaluating the CLPD contribution due to a couple of plane facets sharing a vertex.

with

$$L_V(x) \equiv x \tan(\beta/2) = x/\sqrt{3}. \quad (50)$$

The unit normals are  $\nu_1 = (0, -1, 0)$  and  $\nu_2 = (-\sin \alpha_c, \cos \alpha_c, 0)$  with  $\alpha_c \equiv (\pi - \alpha)$ . After putting  $\theta = \theta' + \pi/2$  and  $\varphi = \varphi' + (\pi + \alpha_c)/2$  (and denoting  $\theta'$  and  $\varphi'$  again by  $\theta$  and  $\varphi$  for notational simplicity) one finds that  $|\theta| < \pi/2$  and  $|\varphi| < (\pi - \alpha_c)/2 = \alpha/2$ . The angular factor  $(\nu_1 \cdot \hat{\omega})(\nu_2 \cdot \hat{\omega}) \sin \theta$  becomes

$$\mathcal{A}_V(\theta, \varphi) = -\cos^3 \theta \cos(\varphi + \alpha_c/2) \cos(\varphi - \alpha_c/2). \quad (51)$$

The Dirac function and the linearity of  $L_V(x)$  makes the evaluation of the  $x$ ,  $z$ ,  $Y$  and  $Z$  integrals straightforward and  $\gamma_V''(r)$  takes the form

$$\gamma_V''(r) = -\frac{1}{\pi V} \int_0^{\pi/2} d\theta \int_0^{\alpha/2} \mathcal{A}_V(\theta, \varphi) F_V(r, \theta, \varphi) d\varphi \quad (52)$$

with

$$F_V(r, \theta, \varphi) \equiv r \left( \min[a(\theta, \varphi) + (\sin \theta)/2, b(\theta, \varphi) - (\sin \theta)/2] + \min[a(\theta, \varphi) - (\sin \theta)/2, b(\theta, \varphi) + (\sin \theta)/2] \right) \quad (53)$$

and

$$a(\theta, \varphi) \equiv \cotg \beta \cos \theta \cos(\varphi + \alpha_c/2) / \sin \alpha_c, \quad (54)$$

$$b(\theta, \varphi) \equiv \cotg \beta \cos \theta \cos(\varphi - \alpha_c/2) / \sin \alpha_c. \quad (55)$$

The integrand of (52) is invariant with respect to each of the following two transformations  $\theta \rightarrow -\theta$  and  $\varphi \rightarrow -\varphi$ . This explains the integration bounds reported in Eq. (52) and the omission of factor 4 at the denominator. Further,  $F_V(r, \theta, \varphi)$  must be positive and this condition will generally make the integration domain smaller than  $\mathcal{D}_V \equiv \{0 < \theta < \pi/2, 0 < \varphi < \alpha/2\}$ . Solving the inequalities implicit in (53) one finds that  $F_V(r, \theta, \varphi)$  is equal to

$$F_{V,A}(r, \theta, \varphi) = 2r[\cot\beta \cos\theta \cos(\varphi + \alpha_c/2)] / \sin\alpha_c \quad (56)$$

within the integration sub-domain

$$\mathcal{D}_{V,A} \equiv \{0 < \theta < \bar{\theta}_{V,R}(\varphi), 0 < \varphi < \alpha/2\} \quad (57)$$

and to

$$F_{V,B}(r, \theta, \varphi) = r[\cot\beta \cos\theta \cos\varphi - \sin\theta \sin(\alpha_c/2)] / \sin(\alpha_c/2) \quad (58)$$

within the integration sub-domain

$$\mathcal{D}_{V,B} \equiv \{\bar{\theta}_{V,R}(\varphi) < \theta < \pi/2, 0 < \varphi < \alpha/2\} \quad (59)$$

with

$$\bar{\theta}_{V,R}(\varphi) \equiv \arctan[\sin(\varphi)/\sqrt{2}]. \quad (60)$$

Both  $F_{V,A}(r, \theta, \varphi)$  and  $F_{V,B}(r, \theta, \varphi)$  must be non negative. One easily verifies that  $F_{V,A}(r, \theta, \varphi) > 0$  within  $\mathcal{D}_{V,FA} = \mathcal{D}_{V,A}$  and that  $F_{V,B}(r, \theta, \varphi) > 0$  within the subset  $\mathcal{D}_{V,FB}$  of  $\mathcal{D}_{V,B}$  defined as

$$\mathcal{D}_{V,FB} \equiv \{\bar{\theta}_{V,R}(\varphi) < \theta < \bar{\theta}_{V,B}(\varphi), 0 < \varphi < \alpha/2\} \quad (61)$$

with

$$\bar{\theta}_{V,B}(\varphi) \equiv \arctan(\cos\varphi). \quad (62)$$

#### 4.1 Constraints and integration domains for $\gamma_V''(r)$

To determine the integration domains of  $F_{V,A}(r, \theta, \varphi)$  and  $F_{V,B}(r, \theta, \varphi)$  one must also require that the  $x$  and  $Y$  values, determined by the vanishing of the arguments of the Dirac function and equal to

$$\bar{x}_V(r, \theta, \varphi) \equiv r \cos\theta \cos(\varphi - \alpha_c/2) / \sin\alpha_c \quad (63)$$

and

$$\bar{Y}_V(r, \theta, \varphi) \equiv r \cos\theta \cos(\varphi + \alpha_c/2) / \sin\alpha_c, \quad (64)$$

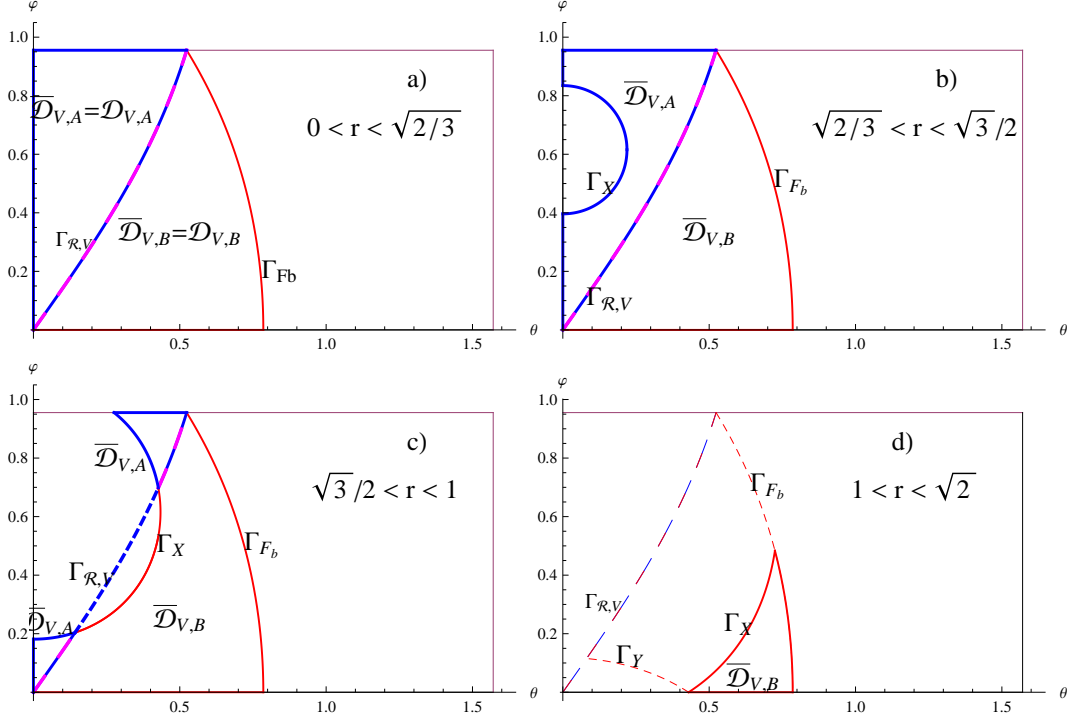


Figure 5: Four panels a), b), c) and d) show the typical shapes of the integration domains  $\bar{\mathcal{D}}_{V,A}(r)$  and  $\mathcal{D}_{V,F_B}(r)$  in the four  $r$  intervals  $a$ ,  $b$ ,  $c$  and  $d$ . The  $\bar{\mathcal{D}}_{V,A}(r)$  domains are bounded by thick blue lines and the  $\bar{\mathcal{D}}_{V,B}(r)$ s by red ones. The dotted thick curve separates  $\mathcal{D}_{V,A}$  from  $\mathcal{D}_{V,B}$ . Curves  $\Gamma_{V,R}$ ,  $\Gamma_{V,x}$ ,  $\Gamma_{V,Y}$  and  $\Gamma_{F_B}$  are respectively defined by Eqs (60), (66), (78) and (62).

respectively, obey constraints (48) and (49), i.e.

$$0 < \bar{x}_V(r, \theta, \varphi) < H \quad \text{and} \quad 0 < \bar{Y}_V(r, \theta, \varphi) < H. \quad (65)$$

The domain  $\mathcal{D}_{V,x}(r)$ , where inequalities (65a) are fulfilled, is determined by curve  $\Gamma_{V,x}(r)$ , defined (where existing) as

$$\Gamma_{V,x}(r) \equiv \{\bar{\theta}_{V,x}(r, \varphi) \equiv \arccos[\sqrt{2/3}/r \cos(\varphi - \alpha_c/2)], \varphi\}, \quad (66)$$

and explicitly reads in the four  $r$ -ranges  $a$ ,  $b$ ,  $c$  and  $d$

$$\mathcal{D}_{V,x,a}(r) = \mathcal{D}_V, \quad (67)$$

$$\mathcal{D}_{V,x,b}(r) = \begin{cases} \{0 < \theta < \pi/2, 0 < \varphi < \bar{\varphi}_{V,x,-}(r)\}, \\ \{\bar{\theta}_{V,x}(r, \varphi) < \theta < \pi/2, \bar{\varphi}_{V,x,-}(r) < \varphi < \bar{\varphi}_{V,x,+}(r)\}, \\ \{0 < \theta < \pi/2, \bar{\varphi}_{V,x,+}(r) < \varphi < \alpha/2\}, \end{cases} \quad (68)$$

$$\mathcal{D}_{V,x,c}(r) = \begin{cases} \{0 < \theta < \pi/2, 0 < \varphi < \bar{\varphi}_{V,x,-}(r)\}, \\ \{\bar{\theta}_{V,x}(r, \varphi) < \theta < \pi/2, \bar{\varphi}_{V,x,-}(r) < \varphi < \alpha/2\}, \end{cases} \quad (69)$$

$$\mathcal{D}_{V,x,d}(r) = \{\bar{\theta}_{V,x}(r, \varphi) < \theta < \pi/2, 0 < \varphi < \alpha/2\}, \quad (70)$$

with

$$\bar{\varphi}_{V,x,\pm}(r) \equiv \alpha_c/2 \pm \arccos(\sqrt{2/3}/r). \quad (71)$$

The  $\mathcal{D}_{V,Y}(r)$  domain, where inequalities (50b) are obeyed, in the four distance sub-ranges is

$$\mathcal{D}_{V,Y,a}(r) = \mathcal{D}_V, \quad (72)$$

$$\mathcal{D}_{V,Y,b}(r) = \mathcal{D}_V, \quad (73)$$

$$\mathcal{D}_{V,Y,c}(r) = \mathcal{D}_V, \quad (74)$$

$$\mathcal{D}_{V,Y,d}(r) = \begin{cases} \{\bar{\theta}_{V,Y}(r, \varphi) < \theta < \pi/2, 0 < \varphi < \bar{\phi}_{V,Y}(r)\}, \\ \{0 < \theta < \pi/2, \bar{\phi}_{V,Y}(r) < \varphi < \alpha/2\} \end{cases} \quad (75)$$

with

$$\bar{\theta}_{V,Y}(r, \varphi) \equiv \arccos[\sqrt{2/3}/(r \cos(\varphi + \alpha_c/2))], \quad (76)$$

$$\bar{\phi}_{V,Y}(r) \equiv -\bar{\varphi}_{V,x,-}(r). \quad (77)$$

## 4.2 $\gamma_V''(r)$ expression

Similarly to subsection 3.2, the  $\gamma_V''(r)$  expression is now given by the sum of the following two expressions

$$\gamma_{V,A}''(r) \equiv -\frac{1}{\pi V \sin \alpha_c} \int_{\bar{\mathcal{D}}_{V,A}(r)} A_V(\theta, \varphi) F_{V,A}(r, \theta, \varphi) d\theta d\varphi \quad (78)$$

$$\gamma_{V,B}''(r) \equiv -\frac{1}{\pi V \sin \alpha_c} \int_{\bar{\mathcal{D}}_{V,B}(r)} A_V(\theta, \varphi) F_{V,B}(r, \theta, \varphi) d\theta d\varphi \quad (79)$$

with

$$\bar{\mathcal{D}}_{V,A}(r) \equiv \mathcal{D}_{V,F_A} \cap \mathcal{D}_{V,x}(r) \cap \mathcal{D}_{V,Y}(r) \quad (80)$$

$$\bar{\mathcal{D}}_{V,B}(r) \equiv \mathcal{D}_{V,F_B} \cap \mathcal{D}_{V,x}(r) \cap \mathcal{D}_{V,Y}(r). \quad (81)$$

The shapes of these domains are shown in Fig. 5 in the four  $r$ -ranges  $a$ ,  $b$ ,  $c$  and  $d$ , defined in the caption of Fig. 5. The integrals were evaluated by the MATHEMATICA. From these follows that the  $\gamma_V''(r)$  expression in the four

$r$ -ranges is

$$\gamma_{V,a}''(r) \equiv (9 + \sqrt{3})r/(96\sqrt{2}), \quad (82)$$

$$\gamma_{V,b}''(r) \equiv -1/(4\sqrt{6}r^3) + 1/(\sqrt{6}r) + (9 - 29\sqrt{3})r/(96\sqrt{2}), \quad (83)$$

$$\begin{aligned} \gamma_{V,c}''(r) \equiv & \frac{1}{192\sqrt{2}\pi r^3} \left[ -8\sqrt{3}\pi + 4r^2 (10\sqrt{3}\pi + 3R_{34}(r) - 4\sqrt{3}\Lambda_c(r)) - \right. \\ & 9(7\sqrt{3} - 2)\pi r^4 + 16\sqrt{3}(4r^2 - 1)\arcsin\left[\frac{7 - 9r^2}{2R_{23}^3(r)}\right] + \\ & 2\sqrt{3}r^4 \left[ 18\arcsin\left[\frac{\sqrt{3}}{2r}\right] + 8\arcsin\left[\frac{2r^2 - 3}{2r^2}\right] + \arcsin\left[\frac{9 - 12r^2 + 2r^4}{2r^4}\right] - \right. \\ & \left. \left. 30\arcsin\left[\frac{7 - 9r^2}{2R_{23}^3(r)}\right] - 24\arcsin\left[\frac{6r^2 - 5}{2R_{23}^2(r)}\right] \right] \right], \quad (84) \end{aligned}$$

$$\begin{aligned} \gamma_{V,d}''(r) \equiv & -\frac{1}{48\sqrt{2}\pi r^3 (3r^2 - 2R_{11}(r))^2} \left[ 3(-16 + 8(12 + \sqrt{3}\pi)r^2 - \right. \\ & 16(5 + \sqrt{3}\pi)r^4 - 2(18 + 5\sqrt{3}\pi)r^6 + 9(3 + 2\sqrt{3}\pi)r^8) - \\ & 6(8 + 12r^2 - 2(31 + 6\sqrt{3}\pi)r^4 + 3(9 + 4\sqrt{3}\pi)r^6)R_{11}(r) + \\ & 2r^2(-4 + 9r^4 + r^2(4 - 12R_{11}(r))) \left[ -2\sqrt{3}\arcsin\left(\frac{4 - 3r^2}{R_{23}^2(r)}\right) + \right. \\ & \left. \left. 3r^2 \left( 3\arcsin\left(\frac{R_{11}(r) - 1}{\sqrt{2}r}\right) + 2\sqrt{3}\arcsin\left(\frac{1}{R_{23}(r)}\right) \right) - 2\sqrt{3}R_{23}^2(r)\Lambda_D(r) \right] \right], \quad (85) \end{aligned}$$

with the following definitions

$$\Lambda_C(r) \equiv \begin{cases} \arcsin\left(\frac{17+18r^2(-2+r^2)}{2R_{23}^4(r)}\right) & \text{if } \sqrt{3}/2 < r < \sqrt{5/6}, \\ -\pi - \arcsin\left(\frac{17+18r^2(-2+r^2)}{2R_{23}^4(r)}\right) & \text{if } \sqrt{5/6} < r < 1, \end{cases} \quad (86)$$

and

$$\Lambda_D(r) \equiv \begin{cases} \arcsin\left(\frac{\sqrt{3}(R_{11}(r)+1)}{2R_{23}(r)}\right) & \text{if } 1 < r < \sqrt{10}/3 \\ \pi - \arcsin\left(\frac{\sqrt{3}(R_{11}(r)+1)}{2R_{23}(r)}\right) & \text{if } \sqrt{10}/3 < r < \sqrt{2}. \end{cases} \quad (87)$$

## 5 Evaluation of $\gamma_P''(r)$

The last case of two parallel facets (see Fig. 6) is now tackled. With the Cartesian frames shown in the figure, facets  $S_1 = DEF$  and  $S_2 = ABC$  are defined by the following inequalities

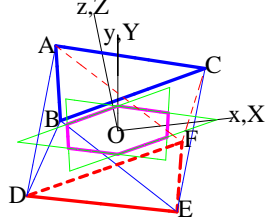


Figure 6: Cartesian frames used for evaluating the CLPD contribution of a couple of plane facets sharing a vertex. The regular hexagon (of side  $1/3$ ) is the orthogonal projection on the plane  $z = 0$  of the facets' portions that are each other parallel.

$$x_m \equiv -2H/3 < x < H/3 \equiv x_M, \quad -L_P(x) < y < L_P(x) \quad (88)$$

$$X_m \equiv -H/3 < X < 2H/3 \equiv X_M, \quad -L_P(-X) < Y < L_P(-X) \quad (89)$$

with

$$L_P(x) \equiv (x + 2H/3) \tan(\beta/2). \quad (90)$$

The unit normals are  $\nu_1 = (0, 0, -1)$  and  $\nu_2 = (0, 0, 1)$  so that the angular factor is

$$\mathcal{A}_P(\theta) \equiv (\nu_1 \cdot \hat{\omega})(\nu_2 \cdot \hat{\omega}) = -\cos^2 \theta. \quad (91)$$

The integrand of  $\gamma_P''(r)$  is  $(\sin \theta \mathcal{A}_P(\theta) \delta(\mathbf{r}_1 + r\hat{\omega} - \mathbf{r}_2))$  with  $\mathbf{r}_1 = (x, y, z)$  and  $\mathbf{r}_2 = (X, Y, Z)$ . The reflection with respect to the plane  $y = 0$  leaves the configuration shown in Fig.6 invariant. Thus, the integrand is left invariant by the transformation  $\varphi \rightarrow (2\pi - \varphi)$ . Hence the  $\varphi$  integral can be restricted to the interval  $[0, \pi]$  provided the result be multiplied by two. The Dirac function fixes the values of  $\theta$ ,  $\varphi$  and  $Y$  as follows

$$\cos \bar{\theta} = h/r, \quad \cos \bar{\varphi} = (X - x)/(r \sin \bar{\theta}) \quad (92)$$

and

$$\bar{Y} = y + r \sin \bar{\theta} \sin \bar{\varphi}. \quad (93)$$



The integral over  $\theta$ ,  $\varphi$  and  $Y$  yields

$$\gamma_P''(r) = - \int_{x_m}^{x_M} dx \int_{X_m}^{X_M} dX \int_{-L_P(x)}^{L_P(x)} dy \frac{\mathcal{A}_P(\bar{\theta}) \Theta_{\bar{P}} \Theta_{\bar{\varphi}}}{2\pi V r^2 \sin \bar{\theta} \sin \bar{\varphi}}, \quad (94)$$

where

$$\Theta_{\bar{P}} \equiv \Theta(L_P(-X) - \bar{Y}) \Theta(L_P(-X) + \bar{Y}), \quad (95)$$

$$\Theta_{\bar{\varphi}} \equiv \Theta(1 - |\cos \bar{\varphi}|), \quad (96)$$

The explicit evaluation of the  $y$  integral gives

$$\gamma_P''(r) = \frac{h^2}{2\pi V r^3} \int_{x_m}^{x_M} dx \int_{X_m}^{X_M} dX \frac{\Theta_{\bar{\varphi}} F_P(r, x, X)}{\Delta(r, x, X)} \quad (97)$$

with

$$\Delta(r, x, X) \equiv \sqrt{r^2 - h^2 - (x - X)^2}, \quad (98)$$

$$\mathcal{M}(x, X, \Delta) \equiv \min[L_P(x) + \Delta/2, L_P(-X) - \Delta/2], \quad (99)$$

and

$$F_P(r, x, X) \equiv \mathcal{M}(x, X, \Delta) + \mathcal{M}(x, X, -\Delta) \quad (100)$$

It is convenient to consider the new integration variables  $(t, u)$ , obtained by a rotation of  $-\pi/4$  of  $(x, X)$ , i.e.

$$x = (t + u)\sqrt{2}, \quad X = (t - u)/\sqrt{2}. \quad (101)$$

The new integration bounds are

$$t_m \equiv -\sqrt{3/8} < t < t_M \equiv \sqrt{3/8} \quad (102)$$

$$u_m(t) < u < u_M(t) \quad (103)$$

with

$$\begin{cases} u_m(t) \equiv t - \sqrt{2/3} & \text{if } t > 0, \\ u_m(t) = u_m(-t) & \text{if } t < 0, \\ u_M(t) \equiv 1/\sqrt{6} - t & \text{if } t > 0, \\ u_M(t) = u_M(-t) & \text{if } t < 0. \end{cases} \quad (104)$$

They are invariant with respect to the exchange  $t \rightarrow -t$  which also implies that  $x \leftrightarrow -X$ . From definitions (98), (92b), (96), (99) and (100) follows that  $\Delta$ ,  $\Theta_{\bar{\varphi}}$  and  $F_P(r, x, X)$  are left invariant by the reflection  $t \rightarrow -t$ . Then (97) becomes

$$\gamma_P''(r) = \frac{h^2}{\pi V r^3} \int_0^{t_M} dt \int_{u_m(t)}^{u_M(t)} du \frac{\tilde{\Theta}_{\bar{\varphi}} \tilde{F}_P(r, t, u)}{\tilde{\Delta}(r, u)}, \quad (105)$$

where the function symbols with the tilde denote the results of the variable change (101) on the corresponding functions without the tilde. The reduction of the inequalities implicit in the  $\tilde{F}_P(r, t, u)$  definition leads to the following two expressions of the integrand (leaving aside the factor  $h^2/\pi V r^3$ ):

$$F_{P,A}(r, t, u) \equiv 2[1 + \sqrt{3/2} (u - t)]/3\tilde{\Delta}(r, u) \quad (106)$$

within the domain

$$\mathcal{D}_{P,A}(r) \equiv \{t > \sqrt{3/2} \tilde{\Delta}(r, u), -\sqrt{(r^2 - h^2)/2} < u < \sqrt{(r^2 - h^2)/2}\} \quad (107)$$

and

$$F_{P,B}(r, t, u) \equiv [2(1 + \sqrt{3/2} u)/3 - \tilde{\Delta}(r, u)]/\tilde{\Delta}(r, u) \quad (108)$$

within the domain

$$\mathcal{D}_{P,B}(r) \equiv \{0 < t < \sqrt{3/2} \tilde{\Delta}(r, u), -\sqrt{(r^2 - h^2)/2} < u < \sqrt{(r^2 - h^2)/2}\}. \quad (109)$$

Both  $\mathcal{D}_{P,A}(r)$  and  $\mathcal{D}_{P,B}(r)$  are subsets of the integration domain  $\mathcal{D}_V$  reported in (105). The above two integrands must be positively valued. Thus one finds that  $F_{P,A}(r, t, u) > 0$  within the domain

$$\mathcal{D}_{P,F_A} \equiv \{t > 0, u > (t - \sqrt{2/3})\} \quad (110)$$

and that  $F_{P,B}(r, t, u) > 0$  within the domain  $\mathcal{D}_{P,F_B}(r)$  that in four  $r$  sub-ranges reads

$$\mathcal{D}_{P,F_B,a}(r) = \emptyset, \quad (111)$$

$$\mathcal{D}_{P,F_B,b}(r) = \{t > 0, -\sqrt{(r^2 - h^2)/2} < u < \sqrt{(r^2 - h^2)/2}\}, \quad (112)$$

$$\mathcal{D}_{P,F_B,c}(r) = \{t > 0, -\sqrt{(r^2 - h^2)/2} < u < \sqrt{(r^2 - h^2)/2}\}, \quad (113)$$

$$\mathcal{D}_{P,F_B,d}(r) = \begin{cases} \{t > 0, -\sqrt{(r^2 - h^2)/2} < u < -(1 + 3\sqrt{r^2 - 1})/2\sqrt{6}\}, \\ \{t > 0, (-1 + 3\sqrt{r^2 - 1})/2\sqrt{6} < u < \sqrt{(r^2 - h^2)/2}\}. \end{cases} \quad (114)$$

The condition  $|\cos \bar{\varphi}| < 1$  is fulfilled within

$$\mathcal{D}_{P,\bar{\varphi}}(r) = \{t > 0, -\sqrt{(r^2 - h^2)/2} < u < \sqrt{(r^2 - h^2)/2}\}. \quad (115)$$

Finally the condition  $|\cos \bar{\theta}| < 1$  requires that the listed domains depending on  $r$  be identified with the void one if  $r < h$ .

In conclusion the final integration domain of  $F_{P,A}(r, t, u)$  is

$$\bar{\mathcal{D}}_{P,A}(r) = \begin{cases} \emptyset & \text{if } 0 < r < h, \\ \mathcal{D}_P \cap \mathcal{D}_{P,A}(r) \cap \mathcal{D}_{P,F_A}(r) \cap \mathcal{D}_{P,\bar{\varphi}}(r) & \text{if } h < r < \sqrt{2}, \end{cases} \quad (116)$$

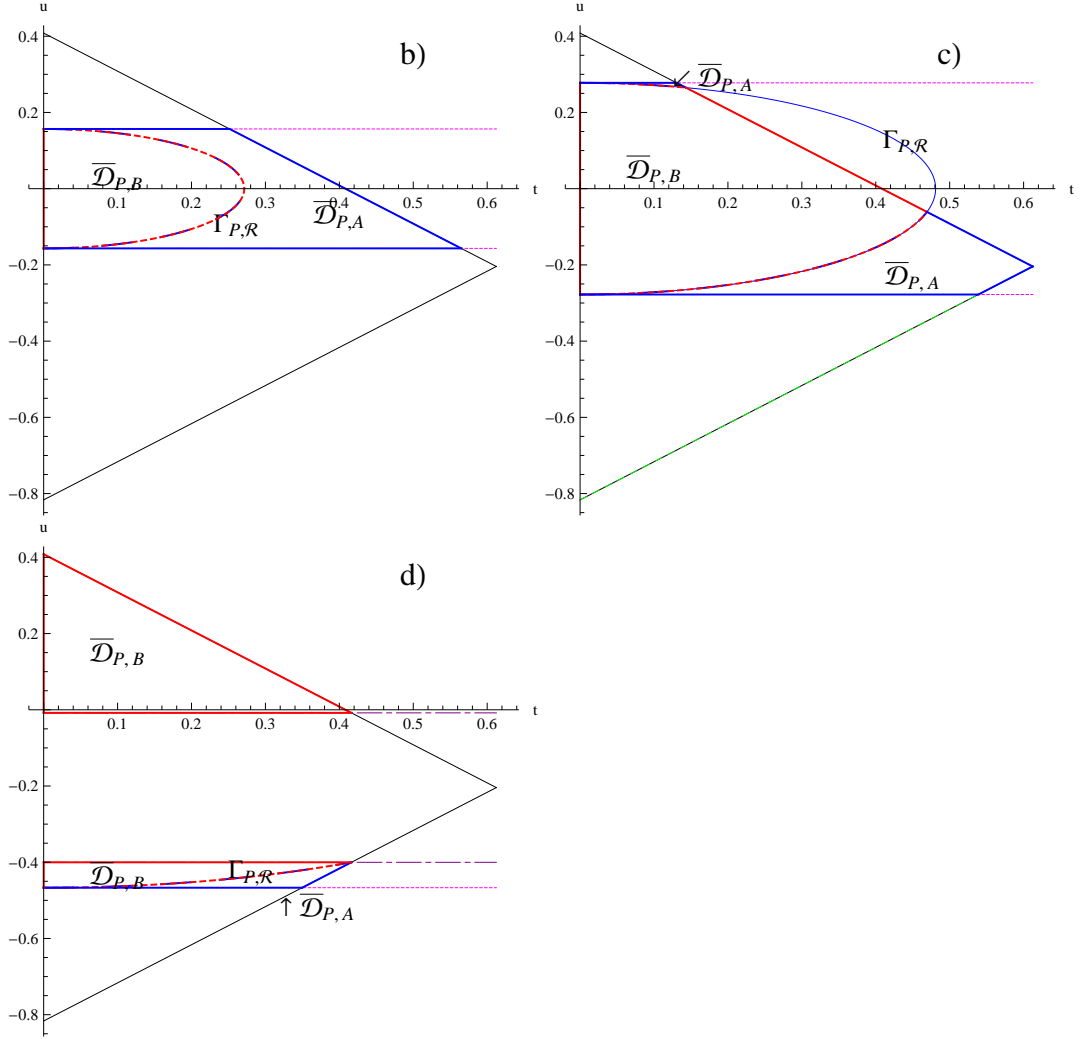


Figure 7: The three panels show the typical shapes of the integration domains  $\mathcal{D}_{P,A}(r)$  and  $\mathcal{D}_{P,B}(r)$  in the  $r$  sub-ranges  $b$ ,  $c$  and  $d$ . The  $\mathcal{D}_{P,A}$  domains are bounded by thick blue lines and the  $\bar{\mathcal{D}}_{P,A}$ s by red ones. The dash-dot thick curve ( $\Gamma_{P,R}$ ) separates the  $\mathcal{D}_{P,A}$  from  $\mathcal{D}_{P,B}$  [see Eq. (107)]. The magenta horizontal dotted lines defines  $\mathcal{D}_{P,\bar{\varphi}}$  [see Eq. (115)]. In case  $d$ , the upper line is not visible because it lies outside  $\mathcal{D}_P$ , while the thin dash-dot purple lines arise from Eq. (114).)

and that of  $F_{P,B}(r, t, u)$  is

$$\bar{\mathcal{D}}_{P,B}(r) = \begin{cases} \emptyset & \text{if } 0 < r < h, \\ \mathcal{D}_P \cap \mathcal{D}_{P,B}(r) \cap \mathcal{D}_{P,F_B}(r) \cap \mathcal{D}_{P,\bar{\varphi}}(r) & \text{if } h < r < \sqrt{2}. \end{cases} \quad (117)$$

The typical shapes of these domains are illustrated in Fig. 7.

### 5.1 $\gamma_P''(r)$ expression

Similarly to subsections 3.2 and 4.2, the  $\gamma_P''(r)$  expression is now given by the sum of the following two expressions

$$\gamma_{P,A}''(r) \equiv -\frac{h^2}{\pi V r^2} \int_{\bar{\mathcal{D}}_{P,A}(r)} F_{P,A}(r, t, u) dt du \quad (118)$$

$$\gamma_{P,B}''(r) \equiv -\frac{h^2}{\pi V r^2} \int_{\bar{\mathcal{D}}_{P,B}(r)} F_{P,B}(r, t, u) dt du. \quad (119)$$

The evaluation of the integrals by the MATHEMATICA yields the  $\gamma_{P,A}''(r)$  and  $\gamma_{P,B}''(r)$  expressions that in turns determine  $\gamma_P''(r)$  in the four  $r$ -ranges as

$$\gamma_{P,a}''(r) \equiv 0, \quad (120)$$

$$\gamma_{P,b}''(r) \equiv \sqrt{3} (1 - r^2) / (2 \sqrt{2} r^3), \quad (121)$$

$$\gamma_{P,c}''(r) \equiv \frac{1}{4\sqrt{2}\pi r^3} \left[ \sqrt{3}\pi - 3 R_{34}(r) - 2\sqrt{3} (2r^2 - 1) \arcsin\left(\frac{1}{2R_{23}(r)}\right) \right], \quad (122)$$

$$\begin{aligned} \gamma_{P,d}''(r) \equiv & -\frac{1}{36\sqrt{2}\pi r^3} \left[ 6\sqrt{3}\pi + (27 - 11\sqrt{3}\pi) r^2 - \right. \\ & 54R_{11}(r) + 6\sqrt{3} (5r^2 - 6) \arcsin\left(\frac{1}{R_{23}(r)}\right) + \\ & \left. 12\sqrt{3} r^2 \arcsin\left(\frac{1 + 3R_{11}(r)}{2R_{23}(r)}\right) \right]. \end{aligned} \quad (123)$$

## 6 $\gamma''(r)$ properties

The expression of  $\gamma''(r)$  immediately follows from (3) and the reported expressions of  $\gamma_E''(r)$ ,  $\gamma_V''(r)$  and  $\gamma_P''(r)$ . The expression is not reported because one does not have a significant cancelation of the addends. The left panel of Fig.8 shows the behaviour of  $\gamma_E''(r)$ ,  $\gamma_V''(r)$  and  $\gamma_P''(r)$  and the right panel that of  $\gamma''(r)$ .

All the functions behave linearly in the innermost  $r$ -range. This result is not surprising because it was since long proved in Ref. [19] that  $\gamma''(r)$  is a linear  $r$ -function in the innermost  $r$ -range whatever the particle shape provided

its boundary is made up of plane facets. The two coefficients of the linear relation are related to the angularity and to the roundness of the particle surface. Further, the explicit expression of the angularity in terms of the edge lengths and the relevant dihedral angles is given by Eq. (4.4) of Ref. [7] and that of the roundness in terms of the dihedral and edge angles by Eq.s (1.7), (3.6), (3.7), (3.14) and (3.11) of Ref. [19]. One easily verifies that the linear coefficients that determine  $\gamma''(r)$  in the  $r$ -range  $a$  coincide with the quoted expressions.

Function  $\gamma''(r)$  shows a finite discontinuity at  $r = \sqrt{2/3}$  that originates from the discontinuity present in  $\gamma_P''(r)$ . The discontinuity is due to the fact that parts of the opposite facets of the octahedron are each other parallel. As shown in Ref.s [12,13], the presence of a parallelism, at a relative distance  $d$ , between subsets of the particle surface is responsible for a discontinuity in  $\gamma''(r)$ . In the case of plane parallel surfaces of area  $S_p$  and distant  $d$ , according to Ref. [12], the discontinuity value is

$$\gamma''(d^+) - \gamma''(d^-) = S_p/(2dV) \quad (124)$$

In the octahedron case,  $S_p$  is the area of the hexagon of side  $1/3$  (see the caption of Fig. 6) and  $d = h$ . Since  $\gamma''(d^+) - \gamma''(d^-) = 8(\gamma_{P,b}''(h) - \gamma_{P,a}''(h))$ , by Eq.s (118) and (119) one verifies that relation (124) is obeyed. Function

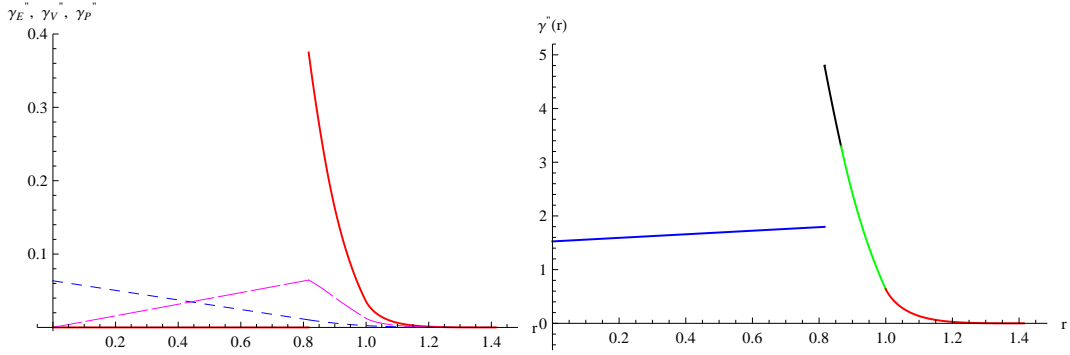


Figure 8: In the left panel the dotted blue curve is the plot of  $\gamma_E''(r)$ , the long dashed magenta curve that of  $\gamma_V''(r)$  and the thick red curve that of  $\gamma_P''(r)$ . The right panel shows the plot of  $\gamma''(r)$  with different colors in the four  $r$ -ranges.

$\gamma''(r)$  must also obey the following sum rules

$$\int_0^\infty \gamma''(r)dr = -\gamma'(0) = S/4V, \quad (125)$$

$$\int_0^\infty r\gamma''(r)dr = \gamma(0) = 1, \quad (126)$$

$$(\pi/3) \int_0^\infty r^4\gamma''(r)dr = 4\pi \int_0^\infty r^2\gamma''(r)dr = V, \quad (127)$$

$$(2\pi/15) \int_0^\infty r^6\gamma''(r)dr = 4\pi \int_0^\infty r^4\gamma''(r)dr = 2R_G^2. \quad (128)$$

The first originates from Porod's law<sup>9</sup>, the second and third from definition (1) of  $\gamma(r)$  and the fourth is related to Guinier's law<sup>2</sup> since  $R_G$  denotes Guinier's giration radius that, in the octahedron case, is equal to  $1/5\sqrt{2}$ . It has been found that the numerical evaluation of the integrals, reported on the left hand sides of (125)-(128), differs, in absolute value, from the right hand side values less than  $8 \times 10^{(-15)}$ .

Using (125) one finds that the chord length probability density of the octahedron is

$$\mathcal{C}(r) = (4V/S)\gamma''(r). \quad (129)$$

The explicit knowledge of  $\gamma''(r)$  allows one to determine numerically both  $\gamma'(r)$  and  $\gamma(r)$  by the relations

$$\begin{aligned} \gamma'(r) &= - \int_r^{\sqrt{2}} \gamma''(t)dt \\ \gamma(r) &= \int_r^{\sqrt{2}} (t-r)\gamma''(t)dt. \end{aligned}$$

Figure 9 shows the resulting plots of  $\gamma(r)$  and  $-\gamma'(r)$ . One observes the well known phenomenon that the particles features become gradually less evident in passing from  $\gamma''(r)$  to  $\gamma(r)$ .

## 7 Conclusion

It has been show that the chord-length probability density of the regular octahedron can algebraically be expressed in terms of elementary functions by separating it into the contributions due to the pairs of the octahedron facets that share a side, a vertex or are each other parallel. The final expressions are somewhat longer than the cube<sup>14</sup> and the tetrahedron ones<sup>18</sup>, *i.e.* the other two Platonic solids for which the  $\gamma''(r)$ s have explicitly been worked out. At

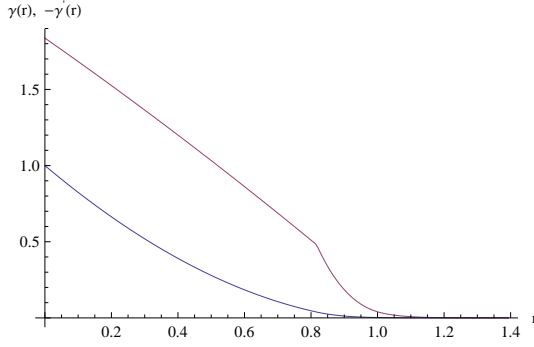


Figure 9: The bottom blue curve is the plot of  $\gamma(r)$  and the top red one that of  $-\gamma'(r)$ .

this point it is not unreasonable to conjecture that the  $\gamma''(r)$ s of all Platonic solids have an algebraic form and, recalling the parallelepiped result<sup>16</sup> as well as the result shown in the two-dimensional case for polygons<sup>20</sup>, the conjecture holds likely true for all polyhedrons.

## Acknowledgment

I thank dr. Wilfried Gille for his critical reading of the ms and for having spotted some misprints.

## References

- <sup>1</sup> P. Debye and A.M. Bueche, *J. Appl. Phys.* **20**, 518, (1949).
- <sup>2</sup> A. Guinier and G. Fournet, *Small-Angle Scattering of X-rays*, (Wiley, New York, 1955).
- <sup>3</sup> L.A. Feigin and D.I. Svergun, *Structure Analysis by Small-Angle X-Ray and Neutron Scattering*, (Plenum Press, New York, 1987).
- <sup>4</sup> P. Debye, H.R. Anderson and H. Brumberger, *J. Appl. Phys.*, **20**, 518, (1957).
- <sup>5</sup> S. N. Chiu, D. Stoyan, W.S. Kendall and J. Mecke, *Stochastic Geometry and its Applications*, (Wiley, Chichester, 3rd Ed. 2013).
- <sup>6</sup> L.A. Santaló, *Integral Geometry and Geometric Probability*, (Addison-Wesley, Reading (MA), 1970).
- <sup>7</sup> S. Ciccariello, G. Cocco, A. Benedetti and S. Enzo, *Phys. Rev. B*, **23**, 6474, (1981).
- <sup>8</sup> S. Ciccariello, *J. Math. Phys.* **36**, 509, (1995).
- <sup>9</sup> G. Porod, *Kolloid Z.* **124**, 83, (1951).
- <sup>10</sup> R. Kirste and G. Porod, *Kolloid Z.* **184**, 1, (1962).
- <sup>11</sup> H. Wu and P. W. Schmidt, *J. Appl. Crystall.* **7**, 131, (1974).
- <sup>12</sup> S. Ciccariello *Acta Crystall. A* **41**, 560, (1985).
- <sup>13</sup> S. Ciccariello, *Phys. Rev. A*, **44**, 2975, (1991).
- <sup>14</sup> J. Goodisman, *J. Appl. Crystall.* **13**, 132, (1980).
- <sup>15</sup> W. Gille, *Exp. Tech. Phys.* **35**, 93, (1987).
- <sup>16</sup> W. Gille, *J. Appl. Crystall.* **32**, 1100, (1999).
- <sup>17</sup> C. Burger and W. Ruland, *Acta Crystall. A* **57**, 482, (2001).
- <sup>18</sup> S. Ciccariello *J. Appl. Crystall.* **38**, 97, (2005).
- <sup>19</sup> S. Ciccariello and R. Sobry, *Acta Crystall. A* **51**, 60, (1995).
- <sup>20</sup> S. Ciccariello, *J. Math. Phys.* **50**, 103527, (2009).